Membrane-Localized Mutations Predict the Efficacy of Cancer Immunotherapy

Priscilla S. Briquez[1+], Sylvie Hauert[1] *, Zoe Goldberger[1,2] *, Trevin Kurtanich[1], Aaron T. Alpar[1], Grégoire Repond[1], Yue Wang[1], Suzana Gomes[1], Prabha Siddarth[3], Melody A. Swartz[1,4,5,6], Jeffrey A. Hubbell[1,5,6+]

* These authors contributed equally to this work

[+] Correspondence: jhubbell@uchicago.edu, pbriquez@uchicago.edu

Affiliations:

[1] Pritzker School of Molecular Engineering, University of Chicago, Chicago, IL, USA

[2] Department of Bioengineering, McGill University, Montreal, QC, Canada

[3] Semel Institute for Neuroscience & Human Behavior, UCLA, Los Angeles, CA, USA

[4] Ben May Department of Cancer Research, University of Chicago, Chicago, IL, USA

[5] Committee on Immunology, University of Chicago, Chicago, IL, USA

[6] Committee on Cancer Biology, University of Chicago, Chicago, IL, USA

SUPPLEMENTARY INFORMATION

Supplementary Data 1: Subcellular locations of proteins associated with *Homo Sapiens* genes.

Supplementary Data 2: Proportion of mutations at specific location for ICI-treated cohort from Samstein *et al.*[7]

Supplementary Data 3: Proportion of mutations at specific location for the non-ICI-treated cohort from Samstein *et al.*[7]

Supplementary Data 4: Proportion of mutations at specific location for the NSCLC patients cohort from Hellman *et al.*[8]

Supplementary Data 5: Proportion of mutations at specific location for the melanoma patients cohort from Hugo *et al.*[9]

Supplementary Data 6: HR of survival per mutated genes and per cancer type for the ICI and non-ICI treated patients cohort from Samstein *et al.*[7]

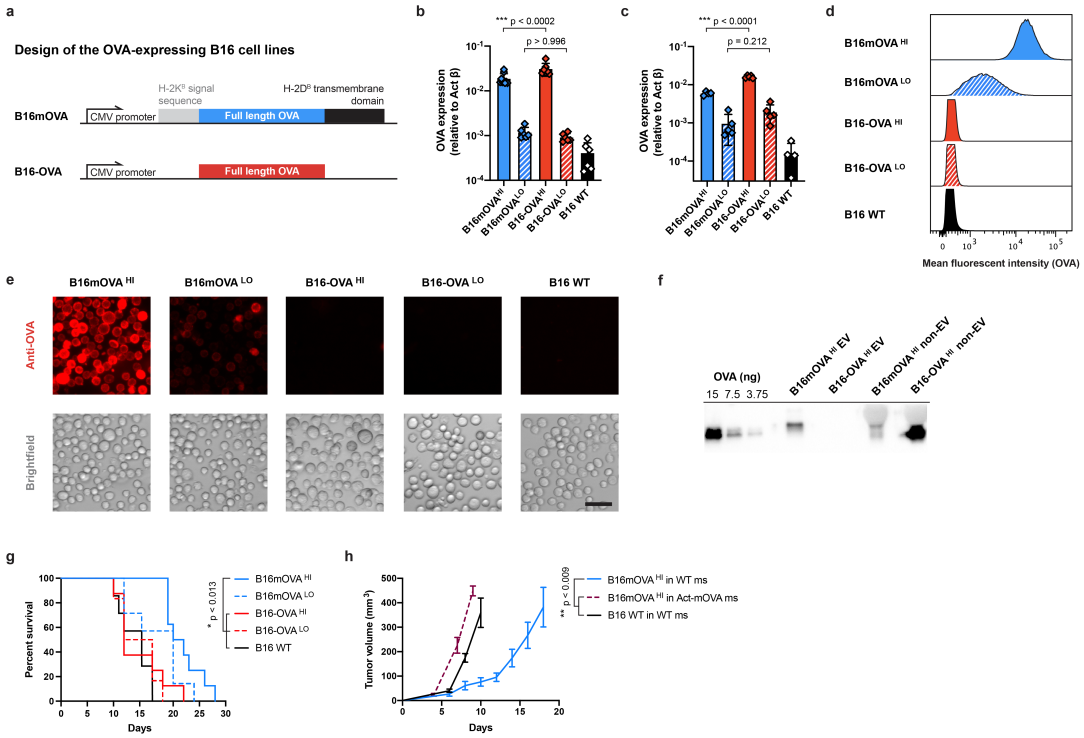

Supplementary Fig. 1. **Characterization of OVA-expressing B16-F10 melanoma cell lines and tumors.** **a,** Design of the different OVA-expressing B16-F10 cell lines, expressing membrane OVA (mOVA) or soluble OVA. **b,** OVA expression in the modified B16 cell lines in culture *in vitro*, assessed by qPCR (N≥6, mean ± SD, ANOVA with Sidak's post-test). **c,** OVA expression in the modified B16 tumors *in vivo*, assessed by qPCR (N≥4, mean ± SD, ANOVA with Sidak's post-test). **d,** Cell-surface staining of OVA quantified by flow cytometry via the mean fluorescence intensity. **e,** Detection of cell plasma membrane-bound OVA on the different OVA-expressing B16 cell lines assessed by microscopy (red: anti-OVA; scale bar = 50 µm). **f,** Western blot analysis for OVA detection in the extracellular vesicles (EV) produced *in vitro* by B16mOVA^{HI} or B16-OVA^{HI} cells lines or in the non-EV fraction (black = positive detection of OVA). **g,** Survival of mice injected with the different OVA-expressing cell lines, associated to the tumor growth curves of Fig. 1a (N≥8, log-rank tests with Holm-Bonferroni p-values adjustment). **h,** Tumor growth of B16mOVA^{HI} in Act-mOVA mice as compared to growth in wild-type (WT) mice (N≥3, mean ± SEM, Kruskal-Wallis with Dunn's post-test at day 10).

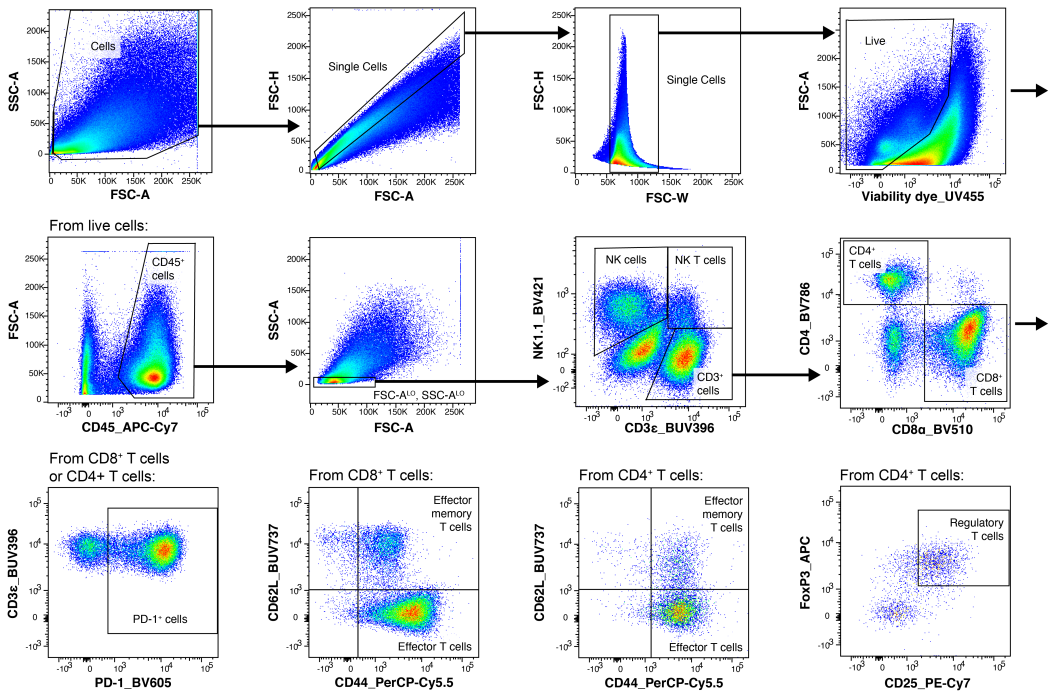

Supplementary Fig. 2. **Gating strategy for the characterization of T and NK cells.** Multi-colored flow cytometry was used to analyze the subsets of T and NK cells in the tumors at day 10 post-injection. Subset of immune cells were defined using the following markers: NK cells (FSC^{LO}, SSC^{LO}, $CD45^+$, $NK1.1^+$, $CD3\varepsilon^-$), NK T cells (FSC^{LO}, SSC^{LO}, $CD45^+$, $CD3\varepsilon^+$, $NK1.1^+$), $CD8^+$ T cells (FSC^{LO}, SSC^{LO}, $CD45^+$, $NK1.1^-$, $CD3\varepsilon^+$, $CD8^+$), CD4+ T cells (FSC^{LO}, SSC^{LO}, $CD45^+$, $NK1.1^-$, $CD3\varepsilon^+$, $CD8^+$), effector T cells (same markers than T cells with $CD44^+$, $CD62L^-$), effector memory T cells (same markers than T cells with $CD44^+$, $CD62L^+$). regulatory T cells (same as $CD4^+$ T cells with $CD25^+$, $FoxP3^+$).

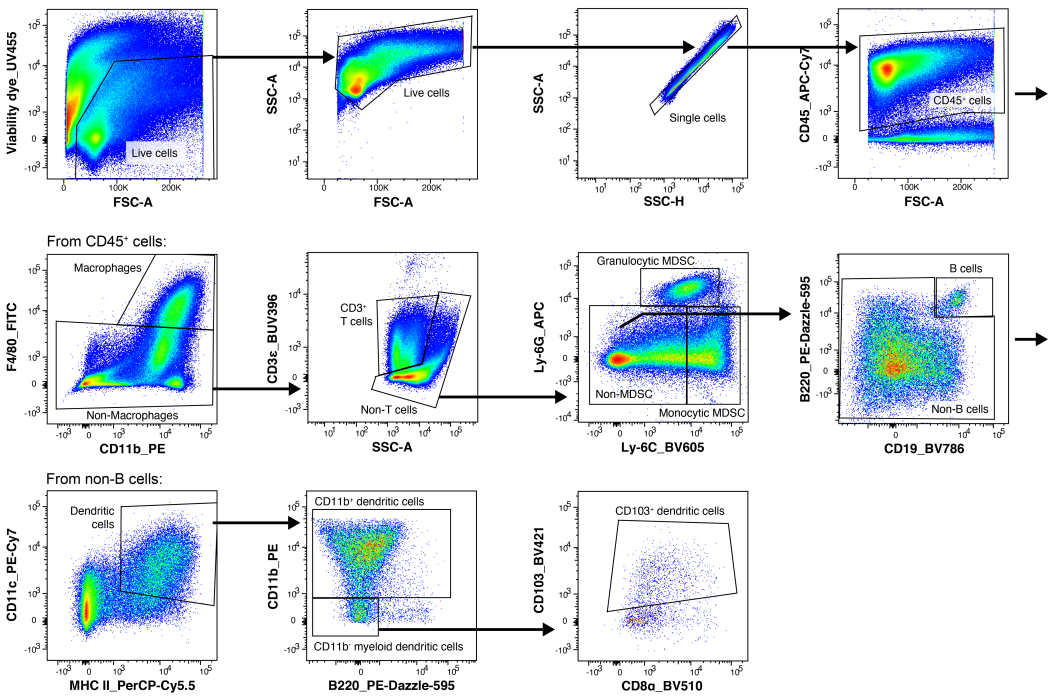

Supplementary Fig. 3. **Gating strategy for the characterization of B cells and myeloid cell subsets.** Multi-colored flow cytometry was used to analyze the subsets of B cells and myeloid cells in the tumors at day 10 post-injection. Subset of immune cells were defined using the following markers: Macrophages ($CD45^+$, $F4/80^+$, $CD11b^+$), Granylocytic myeloid-derived suppressor cells (MDSC) ($CD45^+$, $F4/80^-$, $CD3\varepsilon^-$, $Ly6G^+$, $Ly6C^{MID/HI}$), Monocytic MDSC ($CD45^+$, $F4/80^-$, $CD3\varepsilon^-$, $Ly6G^-$, $Ly6C^{HI}$), B cells ($CD45^+$, $F4/80^-$, $CD3\varepsilon^-$, $Ly6G^-$, $Ly6C^{LO/MID}$, $CD19^+$, $B220^+$), dendritic cells (DCs) ($CD45^+$, $F4/80^-$, $CD3\varepsilon^-$, $Ly6G^-$, $Ly6C^{LO/MID}$, $CD11c^+$, $MHCII^+$), $CD11b^+$ DCs (same than DCs with $CD11b^+$), $CD103^+$ DCs (same than DCs with $CD11b^-$, $B220^-$, $CD103^+$).

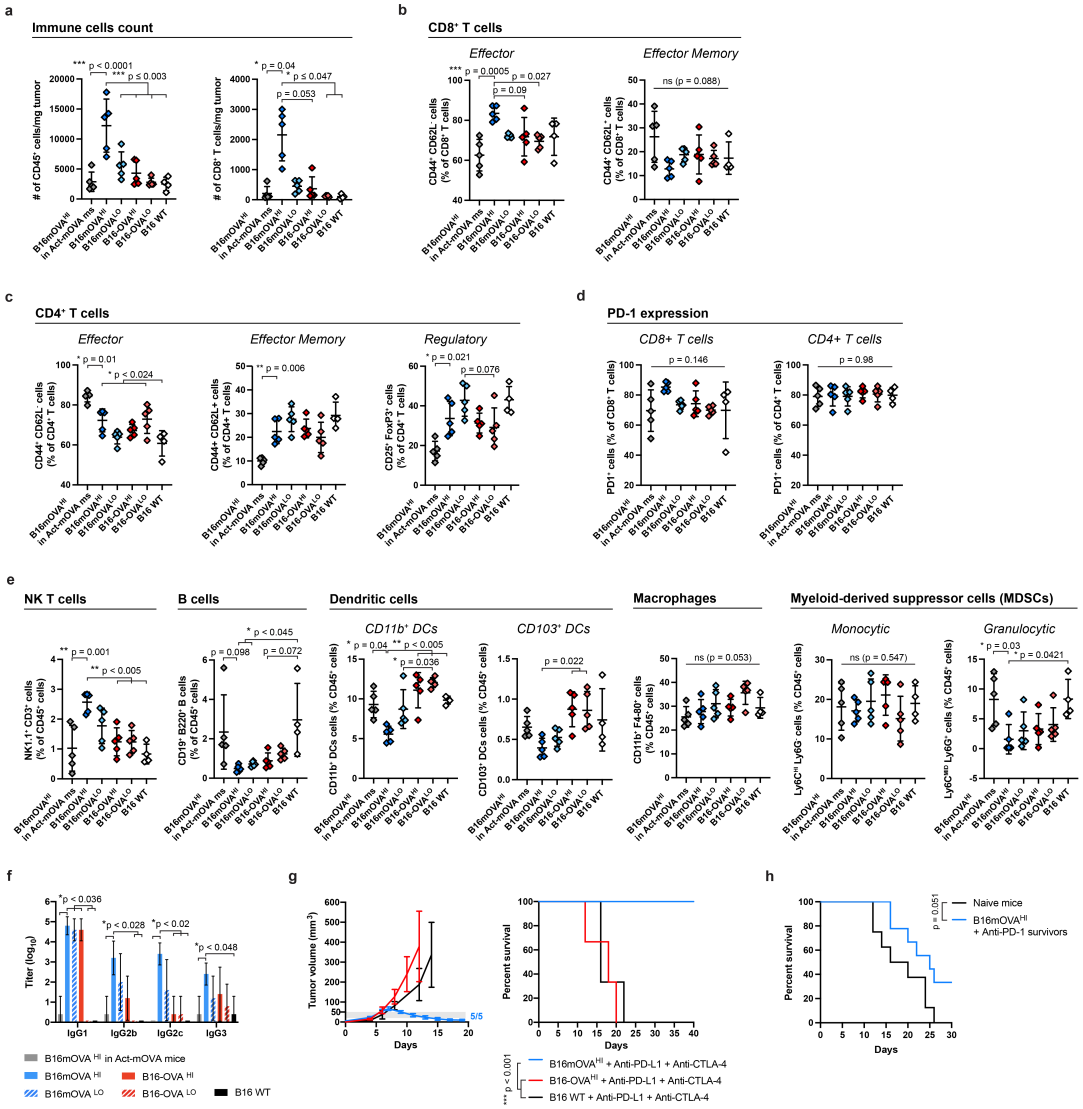

Supplementary Fig. 4. **Comparison of B16mOVA and B16-OVA melanoma tumor immunogenicity and responsiveness to cancer immunotherapy in mice. a-e,** Flow cytometry analysis of immune cells infiltrated in tumors 10 days post-injection (N≥4, mean ± SD, ANOVA with Tukey's post-test and Brown-Forsythe correction when needed). **a,** Number of CD45$^+$ immune cells and CD8$^+$ T cells per mg of tumor. **b,** CD8$^+$ and **c,** CD4$^+$ effector and effector memory T cells subsets in the different tumors. **d,** Proportion of PD-1 expressing CD8$^+$ and CD4$^+$ T cells. **e,** Proportion of NK T cells, B cells, dendritic cells, macrophages and myeloid-derived suppressor cells relative to the total CD45$^+$ immune cell populations. **f,** Titers (log_{10}) of the anti-OVA measured per IgG subtype in the plasma of tumor-bearing mice at day 10, which corresponds Fig. 1d. (N≥4, mean ± SD, Kruskal-Wallis with Dunn's post-test per IgG subtype). **g,** Tumor growth and associated survival of OVA-expressing tumor-bearing mice treated with 100 µg of anti-PD-L1 and 100 µg of anti-CTLA-4 injected intraperitoneally when the tumor volume reached 20-50 mm^3 (grey thresholds) (N≥3, mean ± SEM, log-rank tests). **h,** Survival of mice re-challenged with B16-F10 WT tumor cells, associated to the tumor growth curves presented in Fig. 1i (N≥8, mean ± SEM, log-rank test).

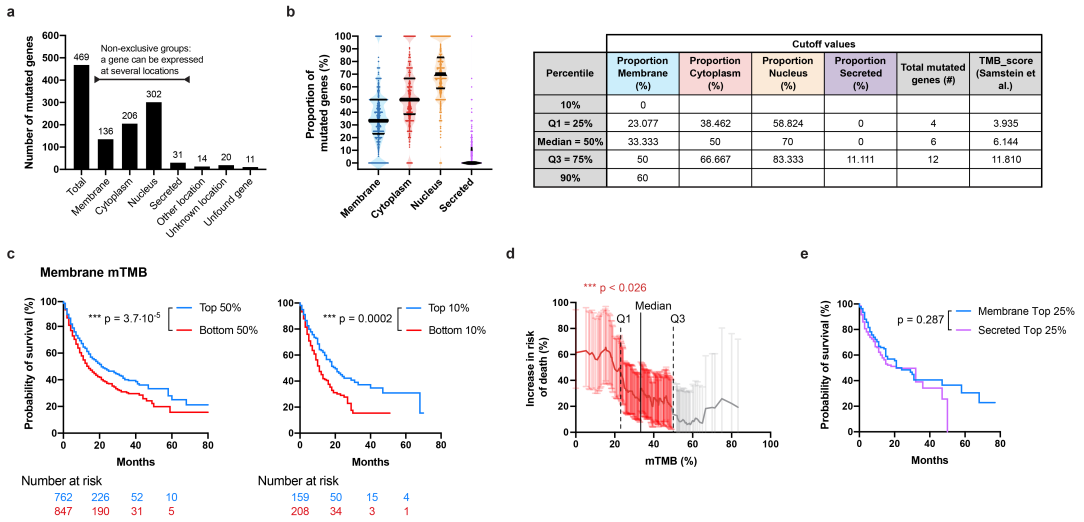

	Cutoff values					
Percentile	Proportion Membrane (%)	Proportion Cytoplasm (%)	Proportion Nucleus (%)	Proportion Secreted (%)	Total mutated genes (#)	TMB_score (Samstein et al.)
10%	0					
Q1 = 25%	23.077	38.462	58.824	0	4	3.935
Median = 50%	33.333	50	70	0	6	6.144
Q3 = 75%	50	66.667	83.333	11.111	12	11.810
90%	60					

Supplementary Data Fig. 5. Analysis of tumor mutated genes' subcellular localizations and their subsequent impact on patient survival. **a,** Number of tumor mutated genes associated with each subcellular location among the 469 genes sequenced by MSK-IMPACT method. **b,** Proportion of tumor mutated genes per subcellular location in patients treated with immunotherapy in the pan-cancer group, and corresponding percentile cutoff values used for the analysis in Fig. 2. **c,** Survival of ICI-treated patients harboring high (Top 50% or 10%) or low (Bottom 50% or 10%) mTMB (log-rank tests). **d,** Increase in risk of death as a function of mTMB in ICI-treated patients in the pan-cancer group. Values are calculated as 100*(HR-1) ± 95% CI with HR the hazard ratio for survival of patients that have less than the depicted proportion as compared to those that have more. As an example, ICI-treated patients that had less than Q1=23% of mutated genes at the membrane had a 50% increased risk of death as compared to those that have more than 23% membrane mutated genes (log-rank tests, red values = p-value ≤ 0.05, grey values = not significant). **e,** Survival of ICI-treated patients with high (Top 25%) mTMB and sTMB (log-rank test).

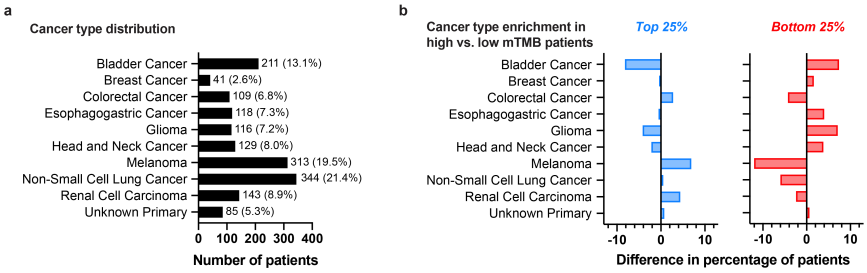

c

Hazard ratio analysis of high vs. low mTMB per cancer type

	THRESHOLD USING UNIVERSAL CUTOFF VALUES					THRESHOLD USING 25% TOP vs. 25% BOTTOM				
	Hazard ratio	95% CI upper limit	95% CI lower limit	p-value	Number of patients Total (bottom vs. top)	Hazard ratio	95% CI upper limit	95% CI lower limit	p-value	Number of patients Total (bottom vs. top)
Pan-Cancer	0.661	0.798	0.547	1.45E-05	832 (404 vs. 428)	0.661	0.798	0.547	1.45E-05	832 (404 vs. 428)
Bladder Cancer	1.192	2.343	0.607	0.6095	104 (84 vs. 21)	0.843	1.449	0.491	0.5369	110 (57 vs. 53)
Breast Cancer	1.949	5.079	0.748	0.1647	26 (17 vs. 9)	1.639	4.261	0.630	0.3061	26 (12 vs. 14)
Colorectal Cancer	1.015	2.732	0.377	0.9768	51 (10 vs. 41)	1.353	2.748	0.666	0.4007	69 (28 vs. 41)
Esophagogastric Cancer	0.562	1.207	0.261	0.1343	75 (46 vs. 29)	0.477	1.090	0.209	0.0731	60 (30 vs. 30)
Glioma	0.785	1.565	0.394	0.4914	71 (58 vs. 13)	1.194	2.004	0.712	0.5013	82 (43 vs. 39)
Head and Neck Cancer	0.792	1.483	0.423	0.4657	73 (48 vs. 25)	0.459	0.863	0.244	0.0135	67 (34 vs. 33)
Melanoma	0.700	1.239	0.395	0.2183	143 (30 vs. 113)	0.827	1.295	0.528	0.4052	175 (95 vs. 80)
Non-Small Cell Lung Cancer	0.826	1.233	0.553	0.3483	156 (62 vs. 94)	0.959	1.394	0.660	0.8277	180 (86 vs. 94)
Renal Cell Carcinoma	0.351	0.690	0.178	0.0015	83 (26 vs. 57)	0.604	1.142	0.319	0.1168	102 (45 vs. 57)

Supplementary Fig. 6. **Distributions of patients by cancer types and according to their mTMB. a,** Distribution of the ICI-treated patients per cancer type included in the pan-cancer analysis. **b,** Differences in patient distribution per cancer type for the groups with high (Top 25%) or low (Bottom 25%) mTMB, as compared to the distribution of the entire ICI-treated cohort as in panel a. **c,** Values of the HRs, 95% confidence intervals, p-value of the log-rank tests and number of patients used in Fig. 3b, for the universal cutoff and the 25% top vs. bottom strategies.

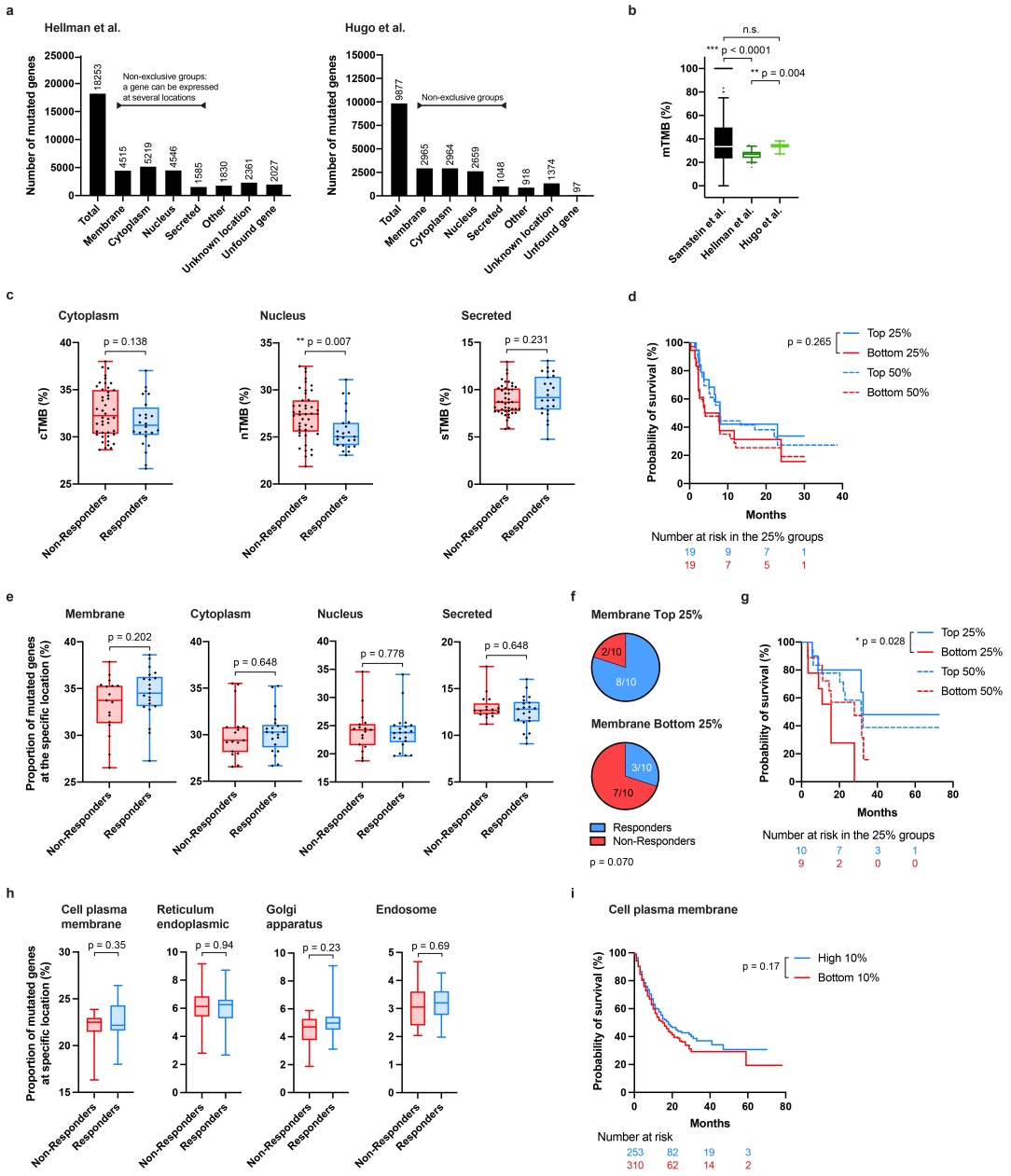

Supplementary Fig. 7. **Response to immunotherapy based on the proportion of mutated genes at specific subcellular localizations.** Patients (N=75) with non-small cell lung cancer were treated with anti-PD-1 + anti-CTLA-4 in the cohort from Hellman *et al.*[8], and patients (N=38) with advanced melanoma cancer were treated with anti-PD-1 in the cohort from Hugo *et al.*[9]. In both studies, tumor mutated genes were sequenced by the WES method. **a,** Number of tumor mutated genes detected across all patients in the Hellman *et al.* and Hugo *et al*. studies, respectively, and their associated subcellular locations. **b,** Comparison of the mTMB found in ICI-treated patient cohorts from the studies by Samstein *et al.*[7], Hellman *et al.*[8] and Hugo *et al.*[9] **c,** Proportion of mutated genes per subcellular location in patients that responded or not to immunotherapy in the Hellman *et al.* cohort (Mann-Whitney test). **d,** Survival of patients with high (Top 25% and 50%) or low (Bottom 25% and 50%) mTMB in the Hellman *et al.*[8] cohort (log-rank test). **e,** Same as in panel c, but with the

patient cohort from Hugo *et al.*[9] **f,** Proportion of responders or non-responders to anti-PD-1 among patients that have high (Top 25%) or low (Bottom 25%) mTMB in the Hugo *et al.*[9] cohort (Fisher's exact test). **g,** Same as in panel d, but with the patient cohort from Hugo *et al.*[9]. **h,** Proportion of mutated genes at the cell plasma membrane or in other specific membrane-containing cell organelles in responders and non-responders to immunotherapy from the Hugo *et al.*[9] **i,** Survival of the patients with high (Top 10%) or low (Bottom 10%) proportion of mutated genes expressing proteins at the tumor cell plasma membrane for the pan-cancer groups from the cohort from Samstein *et al.*[7]

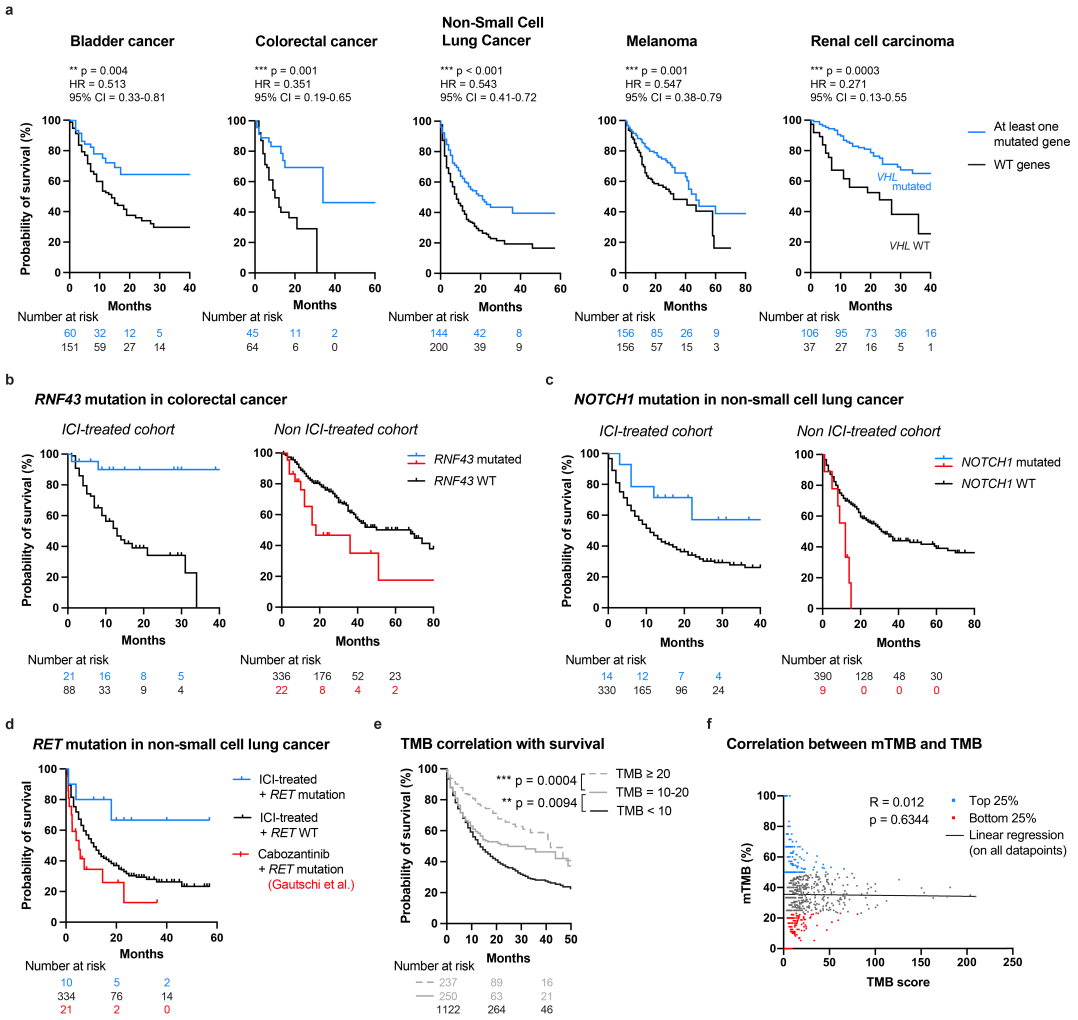

Supplementary Fig. 8. **Potential use of mTMB and specific membrane-associated mutated genes as predictive clinical biomarkers for extended survival upon ICI.** Data analyzed from Samstein *et al.*[7] ICI-treated or non-ICI-treated cohorts. **a,** Survival of patients bearing at least one mutated genes among the cancer-specific list of genes highlighted in blue in Fig. 5a, as compared to patients with no mutated genes among the list. **b,** Survival curves of ICI and non-ICI treated patients bearing *RNF43* mutations in colorectal cancer. **c,** Survival curves of ICI and non-ICI treated patients bearing *NOTCH1* mutations in NSCLC. **d,** Comparison of survival of patients carrying *RET* mutations in NSCLC treated with ICI or with a standard-of-care cabozantinib (data from Gautschi *et al.*[25]). **e,** Survival curves of patients from the pan-cancer group in function of their TMB level (in mut/Mbp). The higher the TMB the longer the survival (log-rank test). f, Correlation between mTMB and total TMB. No correlation was observed between these two parameters (Spearman correlation).